2024 IEEE/ASME International Conference on Advanced Intelligent Mechatronics (AIM)
July 15-19, 2024. Boston, MA, USA

Mechatronic Design of a Thigh-Buttock Analogue and Instrumented Soft Pad for Pressure Injury Prevention

Pat Twomey, Zachary Bravo, and Mitja Trkov

Abstract— **Pressure injuries in immobilized patients pose a global healthcare problem, imposing substantial economic burdens and affecting health and quality of life of those patients. While specialized pressure-redistributing mattresses and contoured foam cushions have been investigated, challenges persist. In this paper, we present mechatronic designs of (i) thigh-buttock (TB) analogue and (ii) instrumented soft pad to study the contact interactions and mechanisms of pressure injury formation in a simulated human body environment. Developed full-scale TB analogue is equipped with embedded vasculature, pressure sensors, and flow sensors, designed to emulate vein collapse dynamics under normal loads. The soft pad is an actively controlled, dynamic, soft support surface discretized into multiple individual actuators with integrated pressure, temperature, and humidity sensors. The integrated sensors allow for continuous monitoring of the contact interactions and environmental conditions at the analogue-pad interface. Effects of developed normalizing pressure distribution algorithm on vein flow at various locations under bony and soft tissues, as well as monitoring of temperature and humidity that are known pressure injury formation factors are demonstrated through extensive experiments. The presented mechatronic design enables controlled physiological simulations contributing towards better understanding of pressure injury mechanisms and potentially leading towards improved pressure injury prevention.**

I. Introduction

Pressure injuries in immobile patients are a pressing concern incurring an economic cost of $26.8 billion annually in the US alone [1]. The existing clinical approaches to prevent pressure injuries, include use of specialized pressure-redistributing mattresses, such as alternating pressures and low-air-loss mattresses [2], [3] that distribute pressure across the mattress-body contact surface, or personalized contoured foam cushions for wheelchair-bound individuals [4]. These foam cushions have been designed based on the developed pressure normalization algorithms [4]. Similar algorithms for normalizing contact pressure distribution have been developed in beds that employ lead screw-driven surface manipulation with integrated force sensitive resistor (FSR) sensors that provide pressure feedback [5]. Other related surface manipulation control approaches have included the use of dielectric elastomers [6] and voice coils-based actuators [7], however, these systems have not been designed for pressure injury prevention.

Recent review summarizing the existing research developments identified limited actuation and sensorized systems to monitor or control pressure, humidity, temperature, or other sensor data for pressure injury prevention applications [8]. Among those, FSR-based pressure mapping and temperature monitoring systems have been demonstrated [9]; however, the sensors were integrated within a rigid surface, which does not allow practical implementation. The usage of FSRs for posture detection in wheelchair-bound individuals [10], [11] has also been used to identify when a user may be in a position making them more susceptible to pressure injuries. Pressure distribution algorithms for ulcer prevention have been proposed [12] employing a human body model to address the limbs and torso individually. However, none of the developed mechatronic systems have been used to experimentally study the blood perfusion under various load conditions on real tissues or anatomical analogues. Investigation of realistic blood perfusion in a testing analogue requires replicating the body hemodynamics. The most important aspect is to replicate the pressure wave and flow generated by the human heart. In the existing literature, the creation of blood pressure waves that mimic the heart pumping patterns have been tested with artificial aortas [13]. A body location specific waves, including in the thigh, have been modeled with pulse width modulation control of peristaltic pumps or piston pumps [14], [15] as a simple alternative approach. Due to complex interaction of many confounding variables, using anatomical analogues could prove useful for testing such instrumented systems and provide insights in understanding of pressure injury risk factors.

In this paper, we present a two part mechatronic system design consisting of (i) an anatomical thigh-buttock (TB) analogue with embedded vasculature and (ii) instrumented soft supporting pad that are used in tandem to study the simulated blood flow in veins flow under various loading conditions and for various anatomical vein locations. The developed instrumented, anatomically matching, soft TB analogue has embedded vasculature, pressure, and flow sensors. The analogue is made of the synthetic materials with matching corresponding bone-muscle-skin tissue structure and mechanical properties. The soft supporting pad design consists of a grid of actuators which design was inspired by our previous work [16], [17] with additionally integrated FSR, humidity, and temperature sensors. The embedded sensors allow monitoring the micro-climate at the contact surface. A normalizing pressure control algorithm was developed to regulate the normal pressure distribution at the TB analogue-soft pad contact surface. The developed TB analogue allows to simulate the complex relationship between flow for various vein depths and locations and at different applied external

This project has been funded in part by a grant from New Jersey Health Foundation (M. Trkov). (*Corresponding author: M. Trkov*).

P. Twomey, Z. Bravo, and M. Trkov are with the Department of Mechanical Engineering, Rowan University, Glassboro, NJ 08028, USA. (e-mail: twomey33@students.rowan.edu, bravoz75@students.rowan.edu, trkov@rowan.edu)

loads, simulating sitting loading condition of a person. The combined system was used to demonstrate the functionality of an actively controlled human-pad interface that can be used either as a combined system for more detailed investigation of confounding variables or separately use the soft pressure pad for potential studies including human subjects to test its practicality and effectiveness thus potentially allow mitigation of risks associated with pressure injury formation.

II. Methods

A. Synthetic Thigh-Buttock Analogue Model

The structure of TB analogue model consists of four main parts representing skin, bone, muscle/fat tissues, and veins. Fig. 1 shows the layout and the inner structure of the model. The TB analogue contains a 3D printed femur and pelvic bone made of PLA+ material (PLA Pro PLA+, e-Sun, China). We chose PLA+ material (Young's Modulus of 3.6 GPa) to represent the bony structures given their stiffness being in the same order of magnitude (Young's Modulus of the femur bone typically ranges between 16.2-19.9 GPa [18], [19]) and cost-effectiveness to easily 3D print bone-shaped structures. The main body of the thigh-buttock is molded from a silicone rubber (Dragon Skin 10A, Smooth-On, Macungie, PA) using a cast thigh from a young male subject (age: 23 years, weight: 66 kg, height: 173 cm). Material hardness is Shore 10 A. An artificial skin (Tattoo skin, Gospire) was used as the most outer layer being glued to the silicone. Six internal silicone tubes (four 1 mm ID and 2 mm OD and four 0.5 mm ID and 2 mm OD, 2 ft long, Quickun, China) where embedded along the length of the model. Diameter of tubes mimicked small veins that were embedded in silicone rubber material positioned under bony structures as well as in the soft tissue to study placement effects under loading. Tubes were connected to two flow sensors (SLF3S-4000B, Sensirion, Switzerland) and two pressure sensors (ABPLANT005PG2A3, Honeywell, US) allowing to perform flow tests in two tubes at the time. Sensors were chosen considering the expected normal blood pressure ranges of general population (75-130 mmHg / 1.2-2.3 psi taken as the maximum range between the Diastolic and Systolic values) [20] and expected mean flow in common (284 mL/min) and superficial (152 mL/min) femoral arteries in the leg [21]. A single peristaltic pump (KPHM400, Kamoer, China) was used to replicate pulsating flow mimicking realistic hemodynamics (i.e., pressure wave and flow) [14].

B. Tube Placement in the Model

In our TB model, silicone tubes were strategically placed under soft tissue or under bony structures to simulate potential vein obtrusion or collapse when subjected to normal loads. This placement aimed to replicate conditions of the transmural load on veins, particularly beneath bony prominences, mirroring scenarios relevant to pressure injury formation. By carefully situating the silicone tubes, simulating mid superficial femoral veins [22], we sought to emulate the anatomical relationship between veins and adjacent bones.

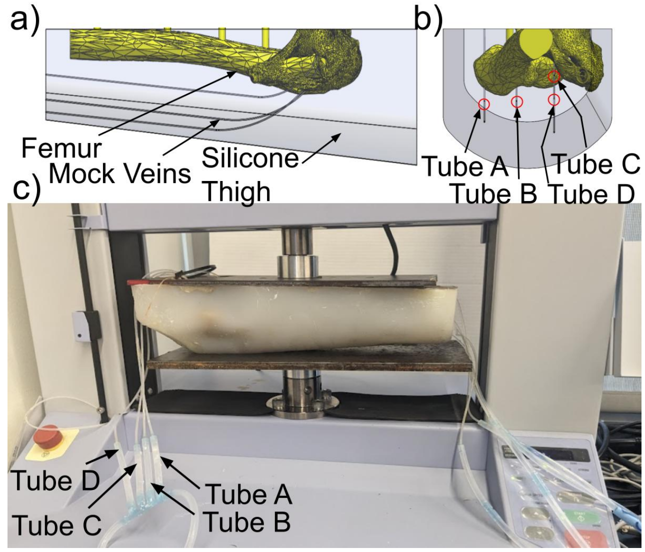

Fig. 1: a) Schematic side view of the thigh-buttock analogue with shown depth of tube placement inside the tissue-bone CAD model. b) Front view of the CAD model with shown tube placement at their exit. c) Experimental setup in a universal testing machine when model is pressed against a flat steel plate.

Therefore, in our study we used only tubes with 1 mm ID. This design choice allowed us to investigate how veins behave under normal loads, potentially providing valuable insights into the dynamics of vein collapse under specific loading conditions.

C. Instrumented Soft Pad Design

The instrumented soft pad comprises of a 2×2 grid (quad) of custom designed soft actuators, each featuring three chambers (two side and one top chamber), as illustrated in Fig. 2a. Each actuator is 50 mm×50 mm×80 mm in size, with a material hardness of Shore 22A, and is molded from dental grade silicone rubber (Elite Double 22, Zhermack, Badia Polesine, Italy), selected specifically due to its inert nature when interfacing with human skin and moisture. The setup was designed to allow modularity by assembling multiple quads into a larger grid forming an IntelliPad structure [17]. Within each actuator, there is a shared pressure sensor, a pressurized air port, and a vacuum port. Selection of the chamber is facilitated by one of three solenoid valves. This set is aid by a fourth solenoid for the selection of the air and vacuum lines. Embedded in each actuator are a thermistor and a force-sensitive resistor (FSR). Data from all sensors on the pad are sampled at 50 Hz sampling frequency. The data was collected on a micro-controller Arduino Mega 2560. Collected data was later post-processed and analysed. Raw FSR data was subsequently converted into load data using a long-short-term memory (LSTM) neural network with 4 hidden layers. The first layer consists of 128 LSTM neurons, followed by a layer of 48 neurons, 24 neurons, 10 neurons, and the output, respectively. Each neuron uses a rectified linear activation function. Each input represents a set of 10 samples with each sample consisting of 4 data points from sensors. The data points are the raw pressure sensors values from the left, right, and top chambers and the raw FSR sensor value. Further details can be found in our related work [23].

During the real-time implementation, the load values for all actuators in the grid are obtained from the analog readings of the FSR sensors. The data is then processed through our load normalization algorithm (see Section II-E). The outputs from the algorithm are sent back to the module to implement the necessary adjustments based on the analyzed data. This process runs continuously when the device is turned on.

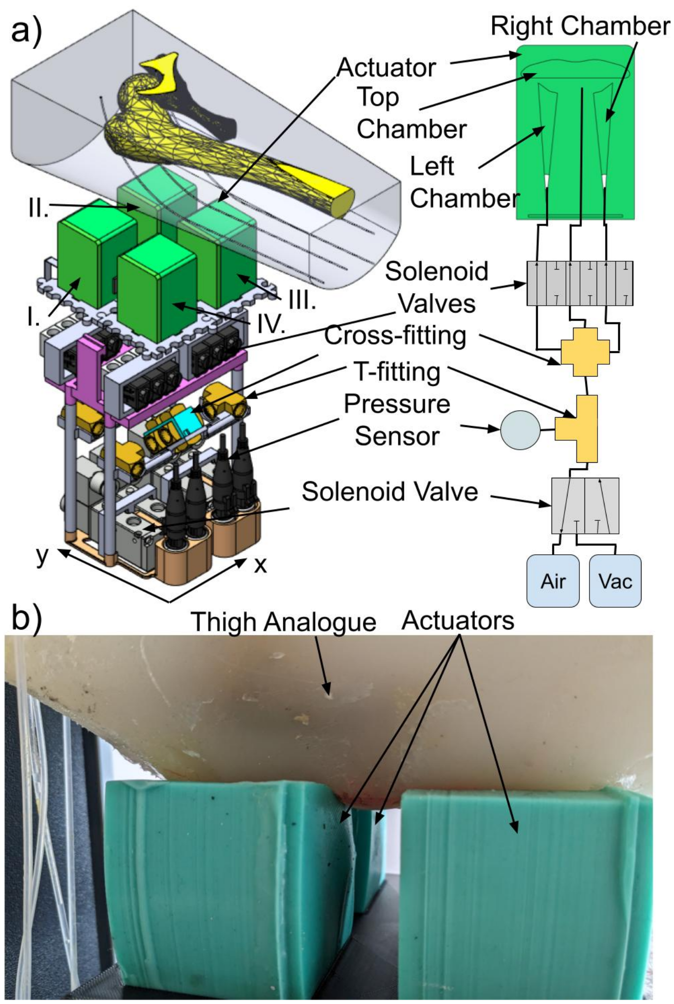

Fig. 2: a) Schematics of the soft pad supporting systems. Detailed CAD design (left) with the corresponding diagram schematics (right) of the pad system used to control the internal air chambers. b) Representation of the actuators during experiments under compression load.

D. Testing of Thigh-Buttock Model

We utilized pulse width modulation (PWM) control on a peristaltic pump to replicate a blood pressure wave [14]. This approach allowed precise modulation of the pump's speed, mimicking the complex dynamics of a femoral blood pressure wave. Through PWM adjustments, we simulated key characteristics such as systolic and diastolic phases, pulse pressure, and pulse duration. However, full hemodynamic replication was constrained by the use of water and viscosity effects in small-diameter tubing [24]. This water-based system introduces deviations from physiological conditions, affecting fluid viscosity and vessel compliance. Despite these limitations, our PWM-controlled peristaltic pump setup provides valuable insights into vein collapse under pulsatile flow conditions, offering a practical compromise for experimental studies within these constraints.

The thigh-buttock analogue was then rigidly mounted to a steel plate and attached to the actuation arm of a universal testing machine (UTM). The purpose is to apply load to the TB model for repeated controlled testing of analogue itself for validation and in combination with our pad of soft actuators. Fig. 1(c) shows the experimental setup of the analogue inside the UTM with connections to the inlets and outlets of the embedded tubes. Fig. 2(b) shows the TB model pressed against the soft actuators.

E. Load Normalization and Flow

Our testing included investigations of effects of a non-uniform and uniform normal pressure distribution on the flow in tubes. A custom gradient-based pressure normalization algorithm was developed and implemented to test these conditions. Fig. 3 shows the algorithm schematics. The algorithm adjusts the pressure in the chambers of the individual actuator to normalize the pressure distribution considering the feedback from the FSR sensors. Initially, the algorithm computes the total load on the pad by summing the pressures readings of all individual actuators. Actuators that have a load greater than 3% of the total load are identified and flagged as loaded (to account for and eliminate potential sensor reading errors). Subsequently, the algorithm identifies and orders the actuators from greatest to lowest loads among the loaded ones. The normalization process focuses on adjusting first the pressure inside the chambers of the actuator with the lowest load. Adjustments are made to the neighboring actuators to the left or right chamber depending on the gradient between each of them. Additionally, adjustments to the top chamber are considered depending on the load gradient between north and south neighboring actuators. A similar approach is taken for the actuator with the greatest load, adjustments are made in the opposite manner deflating the respective chamber.

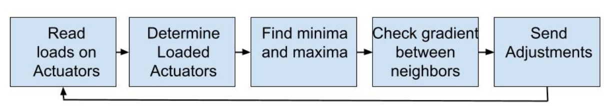

Fig. 3: Pressure normalization algorithm flow diagram.

These adjustments iteratively continue until the standard deviation of all actuators falls below 0.25 N, indicating that approximately 99.7% of loaded actuators are within 0.75 N of each other. In cases where an actuator becomes marked as not loaded, a cleanup function is triggered. This function verifies the pressure of all chambers and readjusts them to a baseline inflation of 5 psi, ensuring a consistent starting point for subsequent measurements. This comprehensive algorithm provides a dynamic and adaptive approach to normalizing pressure distributions.

To evaluate the effectiveness of our normalization algorithm, we conducted experiments using a TB analogue. The analogue was positioned within an UTM equipped with the soft pad system underneath running our normalization algorithm (see Fig. 2(b)). The quad was placed under the bony prominence of the thigh, and UTM was loaded to 270 N. Under controlled static loading conditions, the algorithm dynamically adjusted the pressure distribution within the soft pad, aiming to optimize uniform pressure distribution across the analogue at the contact surface. Through this experimental setup, we were able to observe and analyze the algorithm's impact on the TB's pressure distribution, particularly focusing on its effects on peak blood flows within the simulated TB anatomy.

III. Results

A. Changes in Flow with Uneven Normal Load Distribution

Fig. 4 shows the results of measured peak flows through the tubes during the compression tests, when the analogue was pressed against a flat steel plate (reference test). A pump was set to generate a constant water flow through the tubes. Compression tests at each location were repeated 4 times. Mean and standard deviations for each set of test were computed. We measured the contact area by marking it with a pen when pressed against the steel plate. Knowing the contact area size and the total load we calculated the average pressure ranging from 0 to 37 kPa on the contact surface of the TB analogue.

As load increased, there was a noticeable decreasing trend in the peak flow of water across all tubes. This trend suggests that, on average, the thigh-buttock analogue experiences a reduction in water flow with the increase of pressure/load applied during the compression tests. The lowest ending peak flows of 107.8 ml/min was observed for tube B (see Fig. 1(b)) that was embedded directly under the whole length of the femur bone. Surprisingly, the flow in tube A that was placed directly under the bony prominent structures of the hip ball joint and pelvic bone, respectively, showed higher peak flows compared to tube B that was embedded near tube A running under the full length of the femur bone. The relative peak flow drop in tubes A, B, and C was larger -24 ml/min, -23 ml/min, and -25 ml/min respectively, compared to tube D (-16 ml/min). Relative peak flow reduction was the lowest in tube D (-16 ml/min) that was the most superficial and the furthest away from the bony structures.

B. Normal Load Distribution and Affects on Flow

In the next testing regime, the thigh-buttock analogue was pressed against the non-actuated soft pad. Fig. 5 shows a comprehensive depiction of four repeated compression tests. Pump was commanded to generate same water flow in all tests. The normal load distribution under the TB analogue was measured by the FSR sensors, ranging from 0 to 40 kPa over the course of the test. As expected, the results in Fig 5(a) show a general peak flow reduction as observed

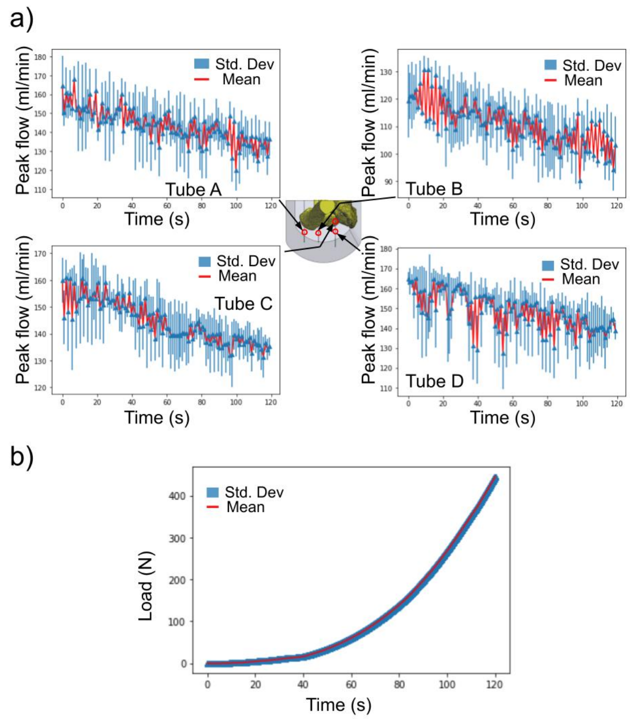

Fig. 4: Results of decreased peak pulsatile flow when increasing the applied normal load on thigh pressed against a steel plate. a) Flow at each tube location. b) Total load on thigh measured by UTM.

in the test when pressed against the flat rigid plate. The relative peak flow drops in tubes A, B, C, and D were -30 ml/min, -12 ml/min, -21 ml/min, and -7 ml/min, respectively. interestingly, the variations in peak flow reduction are greater compared to those when pressed against the flat steel plate, with the larger variations in tube D.

Notably, the greatest load is localized over the bony prominence of the TB's hip joint. Conversely, the more "fatty" section (minimal overlay of bone) of the model experiences relatively less load, likely due to greater compression of the soft tissues.

Fig. 5(b) shows results of a constantly increasing load regimes for each actuators, while Fig. 5(c) shows the overall load of the UTM machine demonstrating same trend. Slight irregularities were observed in load on actuator II, due to bending of the FSR sensor during loading.

In the last series of tests, we investigate the effects of our pressure normalization algorithm on peak flows. Fig. 6 shows results of test where active control of soft pad was applied after the initial static load with uneven pressure distribution. Fig. 6(a) shows starting peak flow pressures similar to those reported at the end of the test in Fig. 5. During this last test, the average contact pressure maintained in a range between 31.2 and 31.5 kPa. During the application of our load normalization algorithm an upward trend indicating increase in peak flows was observed as shown in Fig. 6(a). The application of load normalization shows reducing the pressures applied to the surface under the bony prominence

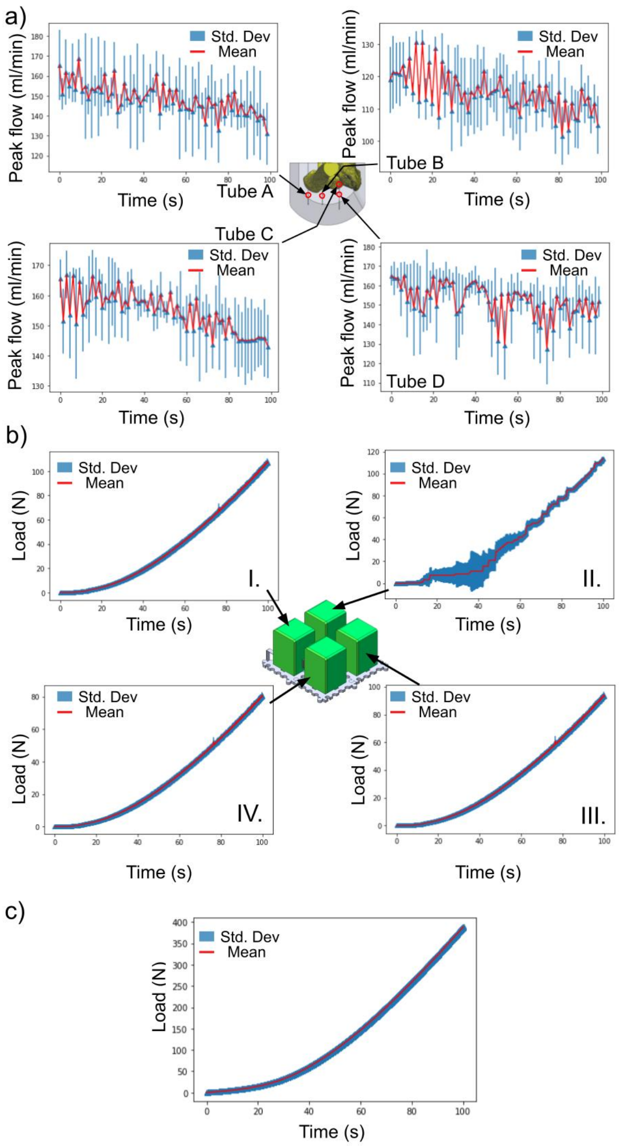

Fig. 5: Results of decreased peak flow, after application of normal load on thigh against soft actuators with no compensation algorithm. a) Plots of flow over time at all four tube locations with means (red) and standard deviations (blue). b) Load on each actuator location, c) Total load on thigh measure by UTM in Newtons.

of the hip joint in the TB shown in Fig. 6(b) as actuator II. The tube under the bony prominence shows the greatest level of improvement in flow post normalization, pointing to the alleviation of pinching by the bone during these tests. Our system and algorithm demonstrated complete pressure normalization across all four actuators as shown in Fig. 6(b) (bottom right), which was achieved in 100 sec time period. The applied overall normal load by the UTM remained constant throughout the test (see Fig. 6(c).

C. Discussion

The observed increase in peak blood flow with the implementation of our pressure distribution algorithm represents a significant outcome in the context of our research. The normalization of contact pressure at the TB model-pad interface facilitated by the algorithm, evidently contributes to an enhanced perfusion. This positive correlation aligns with the intended goal of our soft pad system, aiming to mitigate the risk of pressure injuries. The algorithm's ability to regulate and distribute pressure across the TB surface highlights its potential effectiveness in promoting healthier vascular conditions. The increase in peak blood flow un-

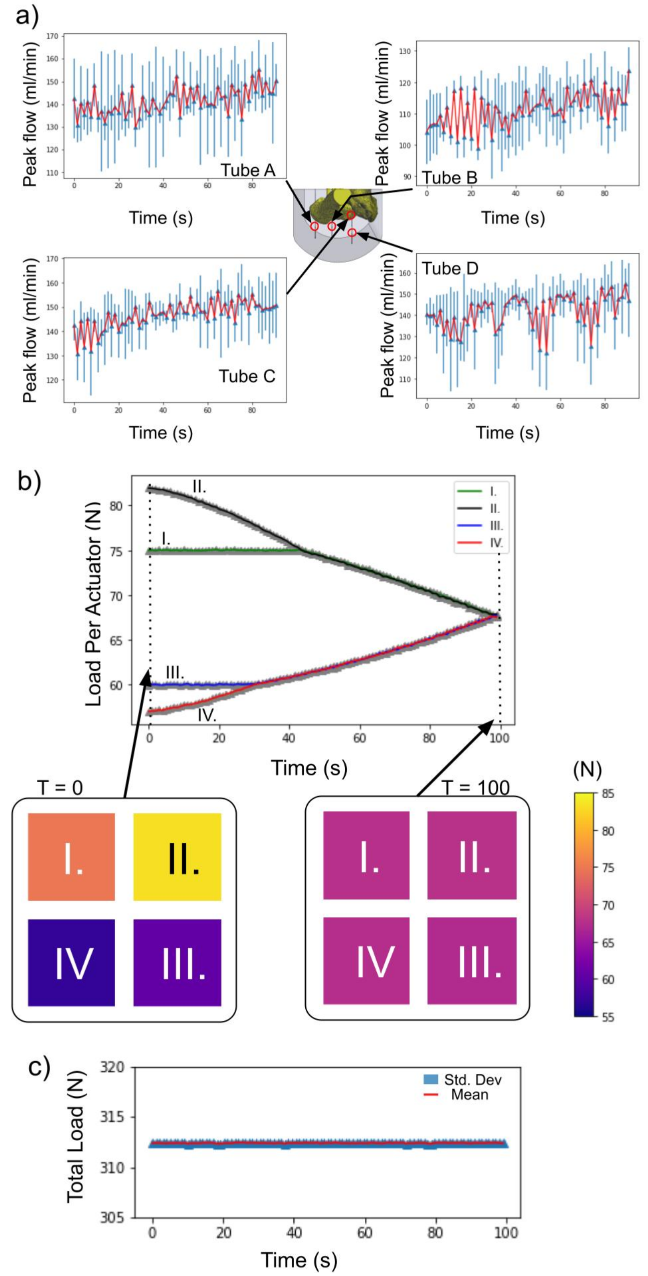

Fig. 6: Results of increase in peak flows after pressing TB model against soft actuators and starting the normal load compensation algorithm. a) Flow through tubes at each location while normalization algorithm is applied. b) Load on each of the actuators as normalization algorithm is applied. c) Total applied load on TB model measured by UTM.

derscores the potential clinical significance of our approach, suggesting a positive impact on circulatory health and, by extension, potential benefits in pressure injury prevention. Further investigations into the specific mechanisms driving this improvement and the system's performance under varied conditions will be crucial for refining the algorithm and maximizing its therapeutic benefits.

IV. Conclusion

In this paper, we outline the development and functionality of an innovative mechatronic system, comprising of a thigh-buttock analogue and an instrumented soft supporting pad. The TB analogue incorporates embedded vasculature and flow sensors, while the soft supporting pad features a grid of soft actuators with integrated FSRs, humidity, and temperature sensors. The integration of these components enables analysis of simulated blood perfusion dynamics and pressure injury prevention under various loading conditions.

In the realm of future work, the integration of specific posture detection holds great potential to enhance the mechatronic system's adaptability. Incorporating posture detection algorithms can allow the system to dynamically adjust its support mechanisms based on the patient's position, optimizing pressure distribution and blood perfusion during various activities. Furthermore, exploring the implementation of wave propagation for deep tissue massage can contribute to therapeutic applications. By incorporating controlled mechanical waves, the system could offer targeted and customizable deep tissue massage to promote circulation and alleviate muscular tension. The addition of shear detection is another avenue for refinement, enabling the system to identify and respond to shear forces acting on the skin. This capability could provide a more comprehensive understanding of the mechanical factors influencing pressure injury formation. Additionally, to ensure the sustained efficacy of the mechatronic system, long-term durability and maintenance considerations are paramount. This validation process will further refine the system's capabilities and contribute to its potential application in diverse clinical settings, thereby advancing the field of pressure injury prevention.

References

[1] C. A. Russo, C. Steiner, and W. Spector, "Hospitalizations related to pressure ulcers among adults 18 years and older, 2006: Statistical brief# 64," 2011.

[2] C. Shi, J. C. Dumville, N. Cullum, S. Rhodes, A. Jammali-Blasi, and E. McInnes, "Alternating pressure (active) air surfaces for preventing pressure ulcers," *Cochrane Database of Systematic Reviews*, no. 5, 2021.

[3] B. Serraes, A. V. Hecke, H. Van Tiggelen, C. Anrys, S. Verhaeghe, and D. Beeckman, "An exploration of nursing home residents' experiences of a non-powered static air mattress overlay to prevent pressure ulcers," *International Wound Journal*, vol. 17, no. 5, pp. 1166–1182, 2020.

[4] S. Li, Z. Zhang, and J. Wang, "Development and evaluation of a new contoured cushion system with an optimized normalization algorithm," *Bio-medical materials and engineering*, vol. 24, no. 6, pp. 3427–3438, 2014.

[5] R. Yousefi, S. Ostadabbas, M. Faezipour, M. Nourani, V. Ng, L. Tamil, A. Bowling, D. Behan, and M. Pompeo, "A smart bed platform for monitoring & ulcer prevention," in *2011 4th international conference on biomedical engineering and informatics (BMEI)*, vol. 3. IEEE, 2011, pp. 1362–1366.

[6] T. Wang, J. Zhang, J. Hong, and M. Y. Wang, "Dielectric elastomer actuators for soft wave-handling systems," *Soft robotics*, vol. 4, no. 1, pp. 61–69, 2017.

[7] R. M. McKenzie, M. E. Sayed, M. P. Nemitz, B. W. Flynn, and A. A. Stokes, "Linbots: Soft modular robots utilizing voice coils," *Soft robotics*, vol. 6, no. 2, pp. 195–205, 2019.

[8] A. Silva, J. Metrôlho, F. Ribeiro, F. Fidalgo, O. Santos, and R. Dionisio, "A review of intelligent sensor-based systems for pressure ulcer prevention," *Computers*, vol. 11, no. 1, p. 6, 2021.

[9] F. F. Daneshvar, S. Moghimi, and R. Lotfi, "Design and evaluation of a pressure and temperature monitoring system for pressure ulcer prevention," *Iranian Journal of Medical Physics*, vol. 11, pp. 242–252, 2014.

[10] C. Ma, W. Li, R. Gravina, and G. Fortino, "Posture detection based on smart cushion for wheelchair users," *Sensors*, vol. 17, no. 4, p. 719, 2017.

[11] M. H. Jaffery, M. A. Ashraf, A. Almogren, H. M. Asim, J. Arshad, J. Khan, A. U. Rehman, and S. Hussen, "Fsr-based smart system for detection of wheelchair sitting postures using machine learning algorithms and techniques," *Journal of Sensors*, vol. 2022, pp. 1–10, 2022.

[12] J. Elfehri, F. Boussu, V. Koncar, and C. Vasseur, "Novel approach of ulcer prevention based on pressure distribution control algorithm," in *2011 IEEE international conference on mechatronics and automation*. IEEE, 2011, pp. 265–270.

[13] J.-H. Jeong, B. Lee, J. Hong, T.-H. Yang, and Y.-H. Park, "Reproduction of human blood pressure waveform using physiology-based cardiovascular simulator," *Scientific Reports*, vol. 13, no. 1, p. 7856, 2023.

[14] S.-M. Jung, G. Y. Chung, and H. S. Shin, "Artificial controlled model of blood circulation system for adhesive evaluation," *Scientific Reports*, vol. 7, no. 1, p. 16720, 2017.

[15] M. Rampazzo, E. Manzoni, M. Lionello, L. Di Micco, and F. M. Susin, "Automation of the peripheral resistance valve in a hydro-mechanical cardiovascular pulse duplicator system," *Control Engineering Practice*, vol. 116, p. 104929, 2021.

[16] M. Raeisinezhad, N. Pagliocca, B. Koohbor, and M. Trkov, "Design optimization of a pneumatic soft robotic actuator using model-based optimization and deep reinforcement learning," *Frontiers in Robotics and AI*, vol. 8, p. 639102, 2021.

[17] ——, "Intellipad: intelligent soft robotic pad for pressure injury prevention," in *2020 IEEE/ASME International Conference on Advanced Intelligent Mechatronics (AIM)*. IEEE, 2020, pp. 685–690.

[18] M. Cuppone, B. Seedhom, E. Berry, and A. Ostell, "The longitudinal young's modulus of cortical bone in the midshaft of human femur and its correlation with ct scanning data," *Calcified tissue international*, vol. 74, pp. 302–309, 2004.

[19] F. Katsamanis and D. D. Raftopoulos, "Determination of mechanical properties of human femoral cortical bone by the hopkinson bar stress technique," *Journal of biomechanics*, vol. 23, no. 11, pp. 1173–1184, 1990.

[20] G. Mancia, R. Sega, C. Bravi, G. De Vito, F. Valagussa, G. Cesana, and A. Zanchetti, "Ambulatory blood pressure normality: results from the pamela study," *Journal of hypertension*, vol. 13, no. 12, pp. 1377–1390, 1995.

[21] C. K. Holland, J. M. Brown, L. M. Scoutt, and K. J. Taylor, "Lower extremity volumetric arterial blood flow in normal subjects," *Ultrasound in medicine & biology*, vol. 24, no. 8, pp. 1079–1086, 1998.

[22] B. S. Hertzberg, M. A. Kliewer, D. M. Delong, K. J. Lalouche, E. K. Paulson, M. G. Frederick, and B. A. Carroll, "Sonographic assessment of lower limb vein diameters: implications for the diagnosis and characterization of deep venous thrombosis." *AJR. American journal of roentgenology*, vol. 168, no. 5, pp. 1253–1257, 1997.

[23] P. Twomey and M. Trkov, "Force, humidity, and temperature estimation of a multi-modal soft actuator for human-pad interface," in *Proc. of 2024 IEEE/ASME International Conference on Advanced Intelligent Mechatronics (AIM)*, Boston, MA, July 2024.

[24] Y.-c. Fung, *Biomechanics: circulation*. Springer Science & Business Media, 2013.